ELSEVIER

Journal of Molecular Structure 611 (2002) 203–211

Journal of
MOLECULAR
STRUCTURE

www.elsevier.com/locate/molstruc

# Torsional vibrational levels combined with higher frequency modes of the jet-cooled *p*-methoxybenzyl alcohol in the $S_1$ excited state

Sun Jong Baek, Daehyun Lee, Kyo-Won Choi, Young S. Choi, Sang Kyu Kim*

*Department of Chemistry, Inha University, Incheon 402-751, South Korea*

Received 10 August 2001; revised 11 March 2002; accepted 11 March 2002

**Abstract**

Resonant two-photon ionization (R2PI) spectrum of *p*-methoxybenzyl alcohol prepared in the supersonic jet has been obtained. Long-progression bands associated with torsional mode of the $CH_2OH$ moiety with respect to the rest of the molecule in the $S_1$ state are observed in the wide spectral range of 35,500–37,500 $cm^{-1}$. The torsional barrier height is found to decrease when the torsional mode is combined with other low-frequency bands at 84 ($\nu_1 = 1$) and 163 ($\nu_1 = 2$) $cm^{-1}$, indicating that this low-frequency mode is modestly coupled to the torsional mode. On the other hand, when the torsional mode is built on the higher-frequency band at 798 ($\nu_2 = 1$) and 1595 $cm^{-1}$ ($\nu_2 = 2$), torsional frequencies are found to be little changed from those located at the origin. Ab initio calculation suggests that this relatively high-frequency mode may be associated with ring-deformation motions, which does not significantly modify the distance and angle between the $CH_2OH$ moiety and aromatic ring. Rotational contour analysis suggests that the transition dipole moment is oriented along the molecular b-axis. The torsional progression bands in the excitation energies higher than ~800 $cm^{-1}$ are found to be much broader than those located at the origin, indicating that intramolecular vibrational redistribution (IVR) becomes quite efficient at such excitation energies.
© 2002 Elsevier Science B.V. All rights reserved.

*Keywords*: *p*-methoxybenzyl alcohol; Torsion; Resonance-enhanced multiphoton ionization; Excited-state; Vibration

## 1. Introduction

Torsional mode spectroscopy has been both extensively and intensively studied for a number of molecules over many decades [1,2]. The torsional mode is intrinsically different from other vibrational modes due to its low vibrational frequency and large amplitude, and has been often treated by hindered internal rotation. For the ground electronic state, infrared or microwave spectroscopy has been widely used in which peak positions split by tunneling have been mainly used as important criteria for determining torsional barrier height. On the other hand, for the electronically excited state, the fluorescence excitation or resonance-enhanced multiphoton ionization (REMPI) spectroscopy employing the supersonic jet and high-resolution lasers has been mostly used for obtaining low-frequency torsional mode spectra [1,2].

Recent researches with regard to torsional spectra have been focused on several subjects including conformational analysis [3–5], the role of torsional mode as a route to fast intramolecular vibrational

* Corresponding author. Tel.: +82-32-860-7688; fax: +82-32-867-5604.

*E-mail address:* skkim@inha.ac.kr (S.K. Kim).

0022-2860/02/$ - see front matter © 2002 Elsevier Science B.V. All rights reserved.
PII: S0022-2860(02)00103-5

redistribution (IVR) process [6–9], and origin of the torsional barrier [10,11]. Toluene and its derivatives belong to the most studied molecules since the internal rotation of the methyl rotor is very well characterized with respect to the benzene ring. For instance, a drastic change in the torsional potential upon the $S_1$–$S_0$ excitation had been observed in the excited spectroscopy of fluorotoluene [10,11], while the direct participation of the methyl rotor in IVR had been demonstrated in the spectroscopic study of *p*-fluorotoluene and 1,4-difluorobenzene molecules [6–8]. Highly resolved excited state spectroscopy of toluene has also been recently reported, elucidating the IVR mechanism that occurs via hyperconjugative interaction between methyl and benzene moieties [9]. However, the coupling mechanism of the torsional mode with other vibrational modes has not been thoroughly investigated yet except for a few cases [12–16]. Though the torsional mode is often treated to be separable from the other higher frequency modes [12,13], the role of torsional mode in IVR and nature of its coupling with other vibrational modes are still not unambiguously known, especially for relatively large molecules which have many vibrational degrees of freedom.

Our group has recently reported the $S_1$-state spectrum of *p*-methoxybenzyl alcohol in the supersonic jet [5]. Torsional motion of the $CH_2OH$ moiety with respect to the rest of the molecule was found to be optically active to give long-progression bands of the corresponding mode. Hole-burning spectroscopy was used to draw a conclusion that only one single conformer of *p*-methoxybenzyl alcohol is present in the jet condition. The spectral analysis was carried out to give the torsional barrier height of 316 $cm^{-1}$ for the $S_1$ ground-vibrational state. In this paper, we revisit the $S_1$-state vibrational spectrum of the same molecule, but this time the spectrum is taken over a much wider spectral range. We have found additional strong torsional progression bands built on the relatively high-frequency ($\sim$800 $cm^{-1}$) vibrational modes. Interestingly, the torsional potential is little affected by this high-frequency vibrational motion, though the IVR becomes quite efficient at such vibrational energies. Meanwhile, the torsional potential is strongly modified when torsion is built on the relatively lower-frequency ($\sim$80 $cm^{-1}$) vibrational mode. Band assignments and associated torsional potentials are given here with the aid of *ab initio* calculation. Low-frequency vibrational modes play an important role in IVR.

## 2. Experimental

The detailed experimental setup was described in Ref. [5]. Briefly, *p*-methoxybenzyl alcohol (Aldrich) supersonically cooled by co-expansion with He or Ar carrier gas through a nozzle orifice (General Valve, 0.5 mm diameter) was prepared in the vacuum chamber. The third harmonic output of a Nd:YAG laser (Spectra-Physics, GCR-150) was used to pump a dye laser (Lumonics, HD-500) to generate the laser output in the 530–564 nm range, followed by the frequency doubling via a BBO crystal placed on an home-made autotracker to give the ultraviolet (UV) laser pulse, which was tunable in the 265–282 nm region. The laser wavelength was calibrated within $\pm 1$ $cm^{-1}$ using the optogalvanic signal from a hollow-cathode lamp (Ne). The UV laser pulse was then overlapped with the molecular beam both in space and time to ionize the title molecule by the (1 + 1) REMPI process. Molecular ions were repelled, accelerated, and drifted along the field-free region until those were detected by a multichannel-plate (MCP, Jordan) to give the REMPI signal. The signal was monitored as a function of the excitation UV wavelength to give REMPI spectra.

## 3. Results and discussion

The REMPI spectrum of *p*-methoxybenzyl alcohol in the jet taken in the 35,500–37,500 $cm^{-1}$ region is shown in Fig. 1. Many peaks corresponding to the $S_1$ vibrational energy levels are observed. Interestingly, the series of bands observed in the 35,700–36,000 $cm^{-1}$ (**I** in Fig. 1) is found to be repeated at $\sim$36,500 $cm^{-1}$ (**II**) and also at $\sim$37,300 $cm^{-1}$ (**III**). There is also another bunch of bands observed between **II** and **III** in Fig. 1. As demonstrated in our previous work [5], each series of bands is due to the torsional motion of the $CH_2OH$ group with respect to the rest of the molecule. For instance, in the series **I**, three torsional progression bands are mixed. One progression is based on the zero-point vibrational energy level, while the other two progression bands

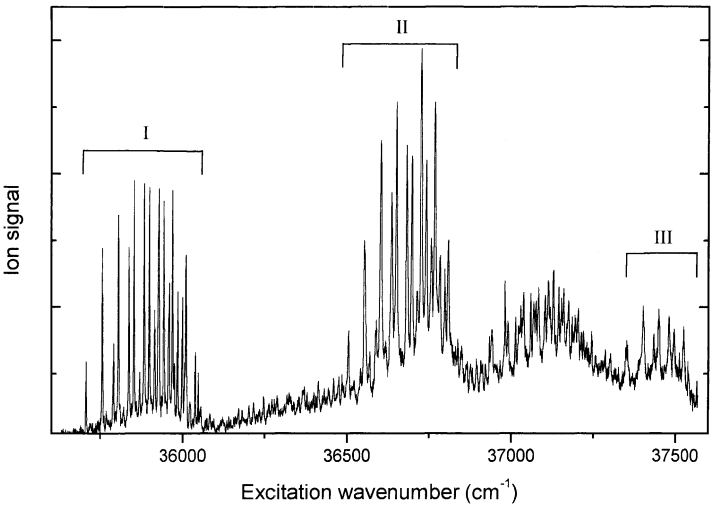


Fig. 1. REMPI ($S_1$–$S_0$) spectrum of *p*-methoxybenzyl alcohol in the supersonic jet taken in the 35,500–37,500 $cm^{-1}$ range. Similar patterns of torsional progression bands are observed in the regions **I**, **II**, and **III**. The increase of broad background is due to both spectral congestion and IVR at high vibrational energies (see the text).

are built on the 84 and 163 $cm^{-1}$ vibrational bands, respectively. Similar patterns are also observed in the series **II** and **III** (Fig. 2).

A sinusoidal function, $V(\phi) = (V_2/2)[1 - cos\ 2\phi]$, is used for torsional potential to construct Hamiltonian, $H = -F(d^2/d\phi^2) + V(\phi)$, where $V_2$ is the torsional barrier height, $F$ is the internal rotational constant, and $\phi$ is the torsional angle. Forty free-rotor wavefunctions are used as a basis set to construct a Hamiltonian matrix, and eigenvalues associated with torsional energy levels are calculated from the matrix diagonalization. It should be noted, however, that only odd overtones of torsional mode are observed since the molecule belongs to $C_{2v}$ group. In Table 1, the torsional barrier height is varied to fit the experiment, giving $V_2 = 316$, 286, and 266 $cm^{-1}$ for the first (+origin), second (+84 $cm^{-1}$), and third (+163 $cm^{-1}$) progression bands in the series **I**, respectively, while $F$ remains constant to be 0.54(5) $cm^{-1}$. In the series **II**, $V_2 =$ 320, 282, and 262 $cm^{-1}$ for those progression bands built on the 798, 884, and 962 $cm^{-1}$ bands, respectively. Similarly, the $V_2$ values are found to be 325 and 286 $cm^{-1}$ for torsional progression bands associated with 1595 and 1681 $cm^{-1}$ bands, respectively, in the series **III** (Table 1). The experimental torsional frequencies are very well reproduced by

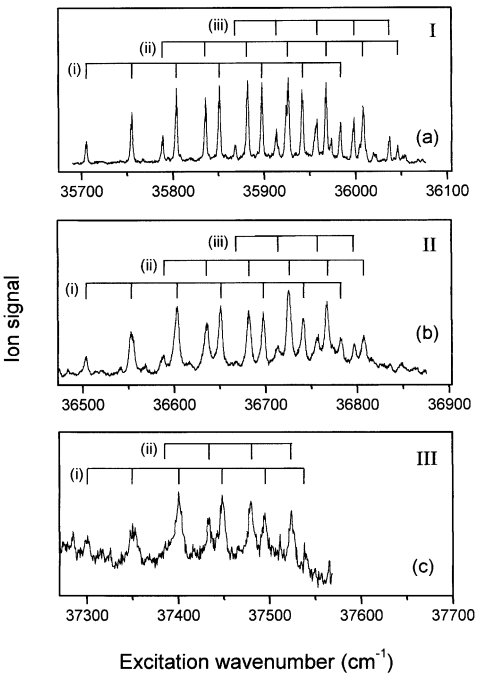


Fig. 2. The $CH_2OH$ torsional progression bands with assignments for: (a) the region **I**, (b) **II**, and (c) the region **III**. The torsional progressions associated with the origin, $\nu_2$, and $2\nu_2$ are denoted as (i), while those combined with $\nu_1$ and $2\nu_1$ are denoted as (ii) and (iii), respectively.

Table 1
Peak positions observed and calculated with assignments

| Peak position ($cm^{-1}$) | $\Delta$ ($cm^{-1}$) | | | | | | Assignment[a] |
|---|---|---|---|---|---|---|---|
| | i | | ii | | iii | | |
| | Exp. | Calcd[b] | Exp. | Calcd[c] | Exp. | Calcd[d] | |
| 35,705 | 0 | 0 | | | | | Origin |
| 35,755 | 50 | 51 | | | | | $2\nu_T$ |
| 35,789 | | | 0(+84) | 0 | | | $\nu_1$ |
| 35,804 | 99 | 100 | | | | | $4\nu_T$ |
| 35,836 | | | 47 | 48 | | | $\nu_1 + 2\nu_T$ |
| 35,851 | 146 | 146 | | | | | $6\nu_T$ |
| 35,868 | | | | | 0(+163) | 0 | $2\nu_1$ |
| 35,882 | | | 93 | 94 | | | $\nu_1 + 4\nu_T$ |
| 35,898 | 193 | 192 | | | | | $8\nu_T$ |
| 35,914 | | | | | 46 | 46 | $2\nu_1 + 2\nu_T$ |
| 35,926 | | | 137 | 137 | | | $\nu_1 + 6\nu_T$ |
| 35,941 | 236 | 236 | | | | | $10\nu_T$ |
| 35,958 | | | | | 90 | 90 | $2\nu_1 + 4\nu_T$ |
| 35,968 | | | 179 | 179 | | | $\nu_1 + 8\nu_T$ |
| 35,983 | 278 | 277 | | | | | $12\nu_T$ |
| 35,999 | | | | | 131 | 132 | $2\nu_1 + 6\nu_T$ |
| 36,008 | | | 219 | 219 | | | $\nu_1 + 10\nu_T$ |
| 36,038 | | | | | 170 | 171 | $2\nu_1 + 8\nu_T$ |
| 36,046 | | | 257 | 255 | | | $\nu_1 + 12\nu_T$ |
| 36,503 | 0(+798) | 0 | | | | | $\nu_2$ |
| 36,553 | 50 | 51 | | | | | $\nu_2 + 2\nu_T$ |
| 36,589 | | | 0(+884) | 0 | | | $\nu_2 + \nu_1$ |
| 36,603 | 100 | 100 | | | | | $\nu_2 + 4\nu_T$ |
| 36,636 | | | 47 | 48 | | | $\nu_2 + \nu_1 + 2\nu_T$ |
| 36,649 | 149 | 147 | | | | | $\nu_2 + 6\nu_T$ |
| 36,667 | | | | | 0(+962) | 0 | $\nu_2 + 2\nu_1$ |
| 36,681 | | | 92 | 93 | | | $\nu_2 + \nu_1 + 4\nu_T$ |
| 36,698 | 195 | 193 | | | | | $\nu_2 + 8\nu_T$ |
| 36,713 | | | | | 46 | 46 | $\nu_2 + 2\nu_1 + 2\nu_T$ |
| 36,725 | | | 136 | 136 | | | $\nu_2 + \nu_1 + 6\nu_T$ |
| 36,741 | 238 | 238 | | | | | $\nu_2 + 10\nu_T$ |
| 36,756 | | | | | 89 | 89 | $\nu_2 + 2\nu_1 + 4\nu_T$ |
| 36,767 | | | 178 | 177 | | | $\nu_2 + \nu_1 + 8\nu_T$ |
| 36,782 | 279 | 280 | | | | | $\nu_2 + 12\nu_T$ |
| 36,797 | | | | | 130 | 130 | $\nu_2 + 2\nu_1 + 6\nu_T$ |
| 36,807 | | | 218 | 217 | | | $\nu_2 + \nu_1 + 10\nu_T$ |
| 37,300 | 0(+1595) | 0 | | | | | $2\nu_2$ |
| 37,350 | 50 | 51 | | | | | $2\nu_2 + 2\nu_T$ |
| 37,386 | | | 0(+1681) | 0 | | | $2\nu_2 + \nu_1$ |
| 37,400 | 100 | 100 | | | | | $2\nu_2 + 4\nu_T$ |
| 37,434 | | | 48 | 48 | | | $2\nu_2 + \nu_1 + 2\nu_T$ |
| 37,448 | 148 | 148 | | | | | $2\nu_2 + 6\nu_T$ |
| 37,480 | | | 94 | 94 | | | $2\nu_2 + \nu_1 + 4\nu_T$ |
| 37,495 | 195 | 194 | | | | | $2\nu_2 + 8\nu_T$ |
| 37,524 | | | 138 | 137 | | | $2\nu_2 + \nu_1 + 6\nu_T$ |
| 37,538 | 238 | 239 | | | | | $2\nu_2 + 10\nu_T$ |

[a] $\nu_T$: $CH_2OH$ torsion, see the text for the $\nu_1$ and $\nu_2$ modes.
[b] $V_2 = 316\ cm^{-1}1$; $F = 0.55\ cm^{-1}$ for the progression bands at the origin, $V_2 = 320\ cm^{-1}$; $F = 0.55\ cm^{-1}$ for those at 36,503 $cm^{-1}$, and $V_2 = 325\ cm^{-1}$; $F = 0.54\ cm^{-1}$ for those at 37,300 $cm^{-1}$.
[c] $V_2 = 286\ cm^{-1}$; $F = 0.54\ cm^{-1}$ for the progression bands at 35,789 $cm^{-1}$, $V_2 = 282\ cm^{-1}$; $F = 0.54\ cm^{-1}$ for those at 36,589 $cm^{-1}$, and $V_2 = 286\ cm^{-1}$; $F = 0.54\ cm^{-1}$ for those at 37,386 $cm^{-1}$.
[d] $V_2 = 266\ cm^{-1}$; $F = 0.54\ cm^{-1}$ for the progression bands at 35,914 $cm^{-1}$, $V_2 = 262\ cm^{-1}$; $F = 0.54\ cm^{-1}$ for those at 36,667 $cm^{-1}$.

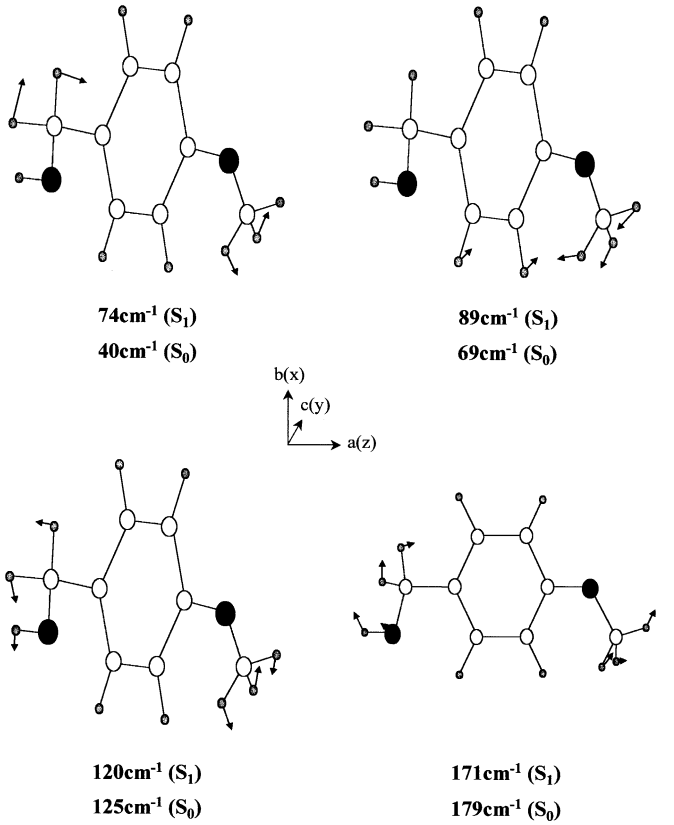


Fig. 3. The ab initio calculated vibrational normal modes of *p*-methoxybenzyl alcohol for the ground (MP2, 6-31G(d)) and excited (CASSCF, 6-31G(d)) states. Four lowest frequency modes are shown. The 74 $cm^{-1}$ ($S_1$) mode corresponds to the $CH_2OH$ torsion. In-plane bending mode at 171 $cm^{-1}$ ($S_1$) is most likely to be responsible for the $\nu_1$ mode.

the above calculation within $\pm 1\,cm^{-1}$. These regular band structures make their assignment quite straightforward; that is, the 84 and 163 $cm^{-1}$ bands are the fundamental and first overtone bands of the mode ($\nu_1$) with $E_{vib} = 84\,cm^{-1}$, respectively. The 798 $cm^{-1}$ band is the fundamental of another vibrational mode ($\nu_2$), while the 1595 $cm^{-1}$ is its first overtone. Accordingly, other pseudo-origins for torsional progression bands located at 884, 962, and 1881 $cm^{-1}$ are assigned to be $\nu_1 + \nu_2$, $2\nu_1 + \nu_2$, and $\nu_1 + 2\nu_2$, respectively. Another series of torsional bands observed in the 36,900–37,300 $cm^{-1}$ region (Fig. 1) are spectrally so congestive, and the assignment has not been tried at this time.

The torsional barrier height decreases when the torsional motion is combined with the $\nu_1$ mode, and it further decreases with two quanta of the $\nu_1$ mode. When the torsional mode ($\nu_T$) is combined with the higher-frequency $\nu_2$ mode, however, the torsional potential is little affected. This indicates that the torsional mode is modestly coupled with the $\nu_1$ mode, while it is effectively isolated from the $\nu_2$ mode. Since the $\nu_1$ mode is coupled to the torsional mode, it may involve nuclear motion which could modify the torsional potential kinetically and/or energetically. Four lowest frequency normal modes, calculated by ab initio for the ground (MP2, 6-31G(d)) and excited (CASSCF, 6-31G(d)) states using a GAUSSIAN 98 program [17] are shown with scaled frequencies in Fig. 3. The $CH_2OH$ torsional mode is calculated to be 74 $cm^{-1}$, which is much higher compared to the experimental value of $\sim$25 $cm^{-1}$. It seems to be that ab initio vibrational

frequencies for the excited state are quite overestimated compared to true values, which could often be the cases particularly for low-frequency modes. The normal modes ($S_1$) calculated to be 89 and 120 $cm^{-1}$ are out-of-plane modes, while the 171 $cm^{-1}$ mode is associated with in-plane nuclear motions (Fig. 3). All the peaks are found out to belong to the b-type transition (vide infra), indicating that the $S_1$ electronic-state belongs to $B_2$ symmetry species. Accordingly, only in-plane vibrational modes of the $S_1$ state are symmetry-allowed for transitions from the ground vibrational $S_0$ state. This symmetry constraint has been well manifested in the absence of even overtones of the out-of-plane $CH_2OH$ torsional mode (Table 1). Though out-of-plane modes could also be optically active when they are combined with odd quanta of the $CH_2OH$ torsional mode, there is little chance for $\nu_1$ to be out-of-plane mode since the peak-intensity variation of torsional progressions with torsional quanta is so similar for all the observed progression bands built on the origin, the $\nu_1$ fundamental, and the first overtone of the $\nu_1$ mode (Fig. 2). In other words, if $\nu_1$ is the out-of-plane mode, the intensity pattern of the torsional progression would vary with the change of its vibrational quantum number, which is not the case here [5]. Therefore, in-plane bending mode calculated at 171 $cm^{-1}$ ($S_1$) seems to be most responsible for $\nu_1$, even though its ab initio frequency is much higher than the experiment. Excitation of the in-plane bending mode should affect the effective torsional potential, since the angle between the $CH_2OH$ and aromatic moieties would be modified significantly.

All the torsional energy levels, even combined with two quanta of $\nu_1$ mode, are so well reproduced by the same torsional potential function just with the variation of the barrier height. Therefore, anharmonic coupling, which would result in the more complex band structures, is less likely to be the main coupling mechanism here. Instead, when the $\nu_1$ mode is combined with $\nu_T$, the torsional barrier height changes due to the torsional-angle dependent vibrational energy of the $\nu_1$ mode. Kinetic energy interaction between $\nu_1$ and $\nu_T$ may also exist though, since the torsional frequency of $\sim$25 $cm^{-1}$ is not so remote from $\sim$80 $cm^{-1}$ for the $\nu_1$ mode. The effective torsional potential depending on the other vibrations had been given as $V_2 = V_2^0 + \Sigma(V'_2)_k\,(\nu_k + 1/2)$ [12], where $V_2^0$ is the electronic contribution with all other coordinates frozen at their equilibrium values and $(V'_2)_k$ represents the energy change associated with nuclear motions of $k$th mode. The above formula, however, does not predict well the dependence of the potential height on vibrational quanta of the $\nu_1$ mode. That is, $(V'_2)_{k=1}$ is obtained as $-30$ or $-20$ $cm^{-1}$ from the comparison of the barrier height for $\nu = 0$ with that for $\nu = 1$ or 2, respectively. Rather, $V_2 = V_2^0 + \Sigma(V'_2)_k\,(\nu_k + 1/2)^{1/2}$ is found to be more consistent with our results (Table 1), giving $(V'_2)_{k=1} = -58$ $cm^{-1}$ for all progression bands. This modified empirical formula works fine for explaining the coupling of $\nu_T$ and $\nu_1$ modes of the title molecule. However, there is no particular dynamical basis in this formula, and the more data on the torsion–vibration coupling for many molecules would be quite helpful to refine the previously suggested empirical formula.

The isolation of $\nu_T$ from $\nu_2$ is quite reasonable, since the torsional motion with $E(\nu_T) \sim 25$ $cm^{-1}$ is much slower than the nuclear motion associated with the $\nu_2$ mode with $E_{vib} = 798$ $cm^{-1}$. Even though a direct dynamic-coupling between $\nu_T$ and $\nu_2$ modes is absent, the expectation value of vibrational energy associated with the $\nu_2$ mode should still be considered as an additional effective torsional potential. However, from the fact that even two quanta of $\nu_2$ do not modify the shape of the effective potential along the torsional angle, it is most likely that the $\nu_2$ mode does not involve the large-amplitude nuclear motion associated with distance or angle between the $CH_2OH$ and aromatic moieties. From the similarity between the experiment and calculation in terms of the vibrational frequency, several plausible ab initio normal modes responsible for the $\nu_2$ mode are shown in Fig. 4. Normal modes at 707 and 950 $cm^{-1}$ ($S_1$) are in-plane modes, while those calculated to be at 757 and 862 $cm^{-1}$ ($S_1$) are associated with out-of-plane nuclear motions. By the same reason used for assigning $\nu_1$ mode (vide supra), out-of-plane modes are ruled out as candidates for the $\nu_2$ mode. Since the $\nu_2$ mode is quite effectively isolated from torsion, the in-plane ring-deformation mode calculated at 950 $cm^{-1}$ ($S_1$), which does not involve the large-amplitude motion associated with the $CH_2OH$ moiety, seems to be the strongest candidate for the $\nu_2$ mode.

In Fig. 5, peak shapes in the region **I** are well

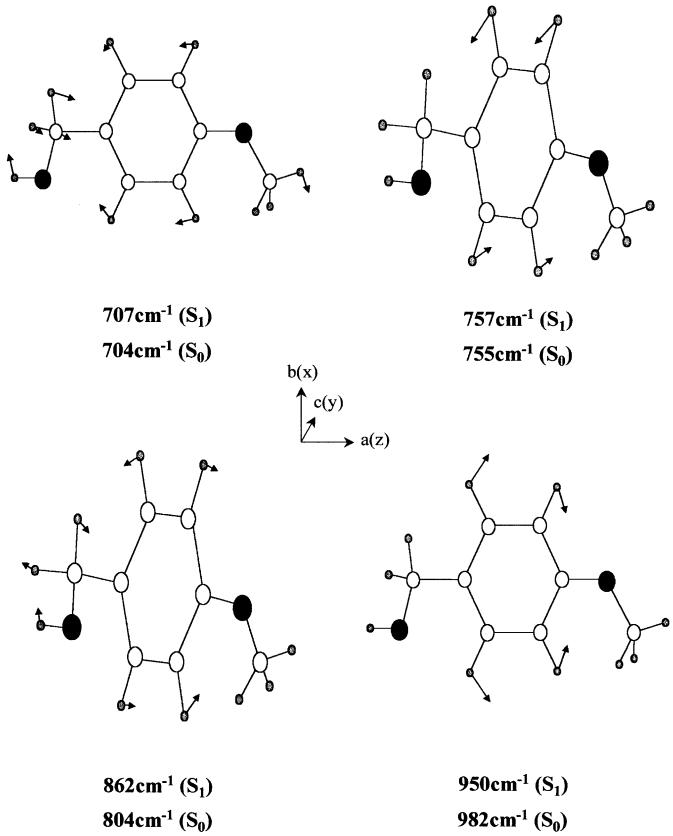


Fig. 4. *Ab initio* vibrational normal modes of *p*-methoxybenzyl alcohol for the ground (MP2, 6-31G(d)) and excited (CASSCF, 6-31G(d)) states. Four normal modes in the 750–1100 $cm^{-1}$ range are shown. In-plane ring-deformation mode at 950 $cm^{-1}$ ($S_1$) is a strong candidate for the $\nu_2$ mode.

reproduced by the simulation using an asymmetric rotor program [18] that carried out for b-type transition with rotational constants of ($A = 3.82\ cm^{-1}$, $B = 0.685\ cm^{-1}$, $C = 0.587\ cm^{-1}$) for both ground and excited states [17]. The laser bandwidth of 0.3 $cm^{-1}$ and rotational temperature of 7 K are used in the simulation. However, in the **II** and **III** regions where the vibrational energy is above ~800 and ~1600 $cm^{-1}$, respectively, the line broadening occurs as clearly shown in Fig. 5(b). Torsional bands in the **II** region are found to be much broader than those in the **I** region, and those are broadened even more in the **III** region. The $S_1$-state lifetime has been estimated to be ~13 ns [5], and its drastic variation upon vibrational excitation, for instance to tens of femtoseconds is not expected. Spectral congestion due to so closely spaced optically bright states other than torsional bands is also not likely, since all the peaks are nicely assigned with torsional progressions (Table 1). Therefore, the line broadening observed in the higher vibrational energy region should be due to coupling of optically bright states with dark states through IVR. The $CH_2OH$ torsional excitation is quite efficient in increasing the density of state with increasing vibrational energy. Thus, this mode should promote the IVR process somehow at high vibrational energies. However, the fact that the $CH_2OH$ torsion is only weakly coupled to high-frequency motions indicates that low-frequency modes other than optically bright torsional mode should be heavily involved in the IVR process. Rotationally resolved spectrum of the title molecule would be very helpful to unravel the nature of the coupling mechanism in the IVR process occurring in the excited state.

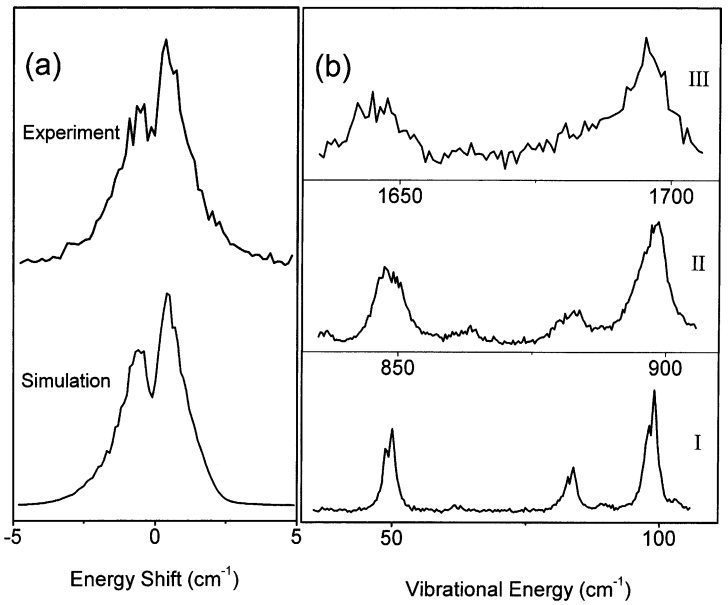


Fig. 5. (a) The experimental line-shape and its simulation using an asymmetric rotor program. The simulation is for the b-type transition. Laser line-width of 0.3 $cm^{-1}$ and rotational temperature of 7 K are used for the simulation. (b) Line-widths of several peaks ($2\nu_T$, $\nu_1$, $4\nu_T$) in the low vibrational energy are compared with those at higher vibrational energy in region **II** ($\nu_2 + 2\nu_T$, $\nu_2 + \nu_1$, $\nu_2 + 4\nu_T$) and **III** ($2\nu_2 + 2\nu_T$, $2\nu_2 + \nu_1$, $2\nu_2 + 4\nu_T$). Line-broadening with increasing the vibrational energy is clearly observed.

## 4. Conclusion

The $S_1$-state torsional spectrum of *p*-methoxybenzyl alcohol in the 35,500–37,500 $cm^{-1}$ range is reported here. The torsion of the $CH_2OH$ group with respect to the rest of the molecule is optically active, and the corresponding long-progression bands combined with other vibrational modes are strongly observed. Torsional mode is modestly coupled with the low-frequency vibrational mode at 84 $cm^{-1}$. This mode makes lower the torsional potential barrier, and should involve the bending motion of the $CH_2OH$ group. Meanwhile, when the torsional mode is combined with the ~800 $cm^{-1}$ band, the barrier height changes little. This experimental fact indicates that the torsion is well isolated from this high-frequency mode, and thus the corresponding nuclear motions are not associated with angle and distance between $CH_2OH$ and aromatic moieties. Mode assignments have been carried out with the aid of ab initio calculation. Line-broadening due to coupling of optically bright states to dark states occurs when the vibrational energy is above ~800 $cm^{-1}$, indicating that IVR is quite efficient at such energies. Low-frequency vibrational motions other than the $CH_2OH$ torsion may play an important role in the IVR process.

## Acknowledgements

This work was financially supported by Korea Research Foundation (Project No. 2000-015-DP0207) and the Brain-Korea 21 program.

## References

[1] J.M. Hollas, D. Phillips (Eds.), Jet Spectroscopy and Molecular Dynamics Chapman & Hall, UK, 1995 Chapter 9.
[2] M. Ito, J. Phys. Chem. 91 (1987) 517.
[3] H.-S. Im, E.R. Bernstein, H.V. Secor, J.I. Seeman, J. Am. Chem. Soc. 113 (1991) 4422.
[4] N. Guchbait, T. Ebata, N. Mikami, J. Am. Chem. Soc. 121 (1999) 5705.
[5] M.-C. Yoon, S.J. Baek, H. Cho, Y.S. Choi, S.K. Kim, J. Phys. Chem. A 104 (2000) 10173.
[6] C.S. Parmenter, B.M. Stone, J. Chem. Phys. 84 (1986) 4710.
[7] D.B. Moss, C.S. Parmenter, G.E. Ewing, J. Chem. Phys. 86 (1987) 51.

[8] Z.-Q. Zhao, C.S. Parmenter, D.B. Moss, A.J. Bradley, A.E.W. Knight, K.G. Owens, J. Chem. Phys. 96 (1992) 6362.
[9] D.R. Borst, D.W. Pratt, J. Chem. Phys. 113 (2000) 3658.
[10] K. Okuyama, N. Mikami, M. Ito, J. Phys. Chem. 89 (1985) 5617.
[11] A. Oikawa, H. Abe, N. Mikami, M. Ito, J. Phys. Chem. 88 (1984) 5180.
[12] C.R. Quade, J. Chem. Phys. 73 (1980) 2107.
[13] P.M. Johnson, T.J. Sears, J. Chem. Phys. 111 (1999) 9222.
[14] L.-H. Xu, J. Chem. Phys. 113 (2000) 3980.
[15] E.C. Richard, R.A. Walker, J.C. Weisshaar, J. Chem. Phys. 104 (1996) 4451.
[16] A. Mcllroy, D.J. Nesbitt, J. Chem. Phys. 101 (1994) 3421.
[17] M.J. Frisch, G.W. Trucks, H.B. Schlegal et al., GAUSSIAN 98, Revision A.6. Gaussian, Inc., Pittsburgh, PA, 1998.
[18] F.W. Birss, D.A. Ramsay, Comput. Phys. Commun. 38 (1984) 83.